J. Geophys. 44, 165–172, 1977

Journal of Geophysics

Measurement of the $O_2(^1\Delta_g)$ Height Profile during a Winter Anomaly Event

W. Bangert[1] and V. Amann[2]

[1] Meteorologisches Institut der Universität München, Abteilung für Atmosphärische Strahlung und Satellitenmeteorologie, Barbarastr. 16, D-8000 München 40, Federal Republic of Germany
[2] Deutsche Forschungs- und Versuchsanstalt für Luft- und Raumfahrt, Institut für Nachrichtentechnik, D-8031 Oberpfaffenhofen, Federal Republic of Germany

Abstract. The emission height profile of the Infrared Atmospheric Band of oxygen at 1.27 μm has been measured at Arenosillo, Spain on January 4, 1976 during a winter anomaly event. The instrument as well as the method of data evaluation are described. Preliminary results for the derived $O_2(^1\Delta_g)$ and O_3 profiles between 40 and 100 km are presented. They show largely enhanced concentrations below 52 km which are assumed to be related to the observed stratospheric warming. Distinct structures at 72, 93, and 100 km are attributed to respective structures in the temperature profile.

Key words: Airglow – Infrared atmospheric bands – $O_2(^1\Delta_g)$ profile – Ozone profile – Winter anomaly.

1. Introduction

Oxygen in the first electronically excited state $^1\Delta_g$ is one of the most abundant minor constituents throughout the mesosphere and lower thermosphere. With an excitation energy of 0.98 eV it is capable of participating in many processes which are important for the photochemistry of the neutral and ionized atmosphere. The measurement of the $O_2(^1\Delta_g)$ concentration height profile may therefore yield a lot of information about the composition of the atmosphere especially when combined with measurements of other constituents like atomic and molecular oxygen and of the temperature profile.

The radiative transition from the $^1\Delta_g$ to the ground state $^3\Sigma_g^-$ gives rise to the emission of the Infrared Atmospheric Band System of oxygen. The strongest band of this system under atmospheric conditions is the vibrational (0,0) transition at 1.27 μm. This emission represents the most prominent feature of the day airglow. Despite this fact it is not easily observed from the ground because of very strong self-absorption in the lower atmosphere. The first observations of the Infrared Atmospheric Band System were therefore those of the (0,1) transition at 1.58 μm reported by Vallance Jones and Harrison (1958).

Subsequent measurements of the 1.27 μm band from baloons and rockets revealed the principal behavior of this emission. During the day there is a strong layer centred near 50 km sloping off nearly exponentially with altitude. Most observations show a secondary peak between 80 and 90 km. The total overhead intensity is typically 25 to 30 MR. After sunset the main and the secondary layers decay except for a remaining intensity of roughly 100 kR centred in one or even two layers around 90 km.

The photochemical reaction scheme capable of explaining the twilight and dayglow observations was first proposed by Gattinger and Vallance Jones (1966). $O_2(^1\Delta_g)$ is produced predominantly by photolysis of ozone by solar radiation in the Hartley continuum:

$$O_3(^1A)+h\nu \rightarrow O_2(^1\Delta_g)+O(^1D) \quad (1)$$

the dissociation coefficient beeing $J_3=9.6\ 10^{-3}\ s^{-1}$ (Ackerman, 1971). Deactivation occurs via spontaneous emission:

$$O_2(^1\Delta_g)\rightarrow O_2(^3\Sigma_g^-)+h\nu \quad (2)$$

with an Einstein transition probability coefficient $A=2.58\ 10^{-4}\ s^{-1}$ (Badger et al., 1965) and collisional quenching by air molecules:

$$O_2(^1\Delta_g)+M\rightarrow O_2(^3\Sigma_g^-)+M \quad (3)$$

with a coefficient $k_1=4.4\ 10^{-19}\ cm^3s^{-1}$ (Clark and Wayne, 1969). The time constant for this mechanism $\tau=(A+k_1\ M)^{-1}$ is smaller than 1 h especially at heights below 75 km where quenching becomes dominant. Thus, photochemical equilibrium can be assumed which means that time dependent as well as flux terms in the continuity equation can be neglected. The processes (1), (2), and (3) therefore lead to the simple equation:

$$(A+k_1[M])\,[O_2(^1\Delta_g)]=J_3[O_3]. \quad (4)$$

Using Eq. (4) the O_3 concentration profile can easily be calculated from a measured profile of the $O_2(^1\Delta_g)$ concentration taking the atmospheric density profile from a model atmosphere or from a simultaneous measurement. This scheme has been shown by Evans et al. (1968) to give quite reasonable agreement with O_3 profiles measured by different methods for heights below the mesopause. For higher altitudes there are discrepancies which lead to the conclusion that further production processes besides ozone photolysis must be operating. These might be at least partly the same as those producing the nightglow emission of appr. 100 kR but have not been identified as yet. Therefore O_3 profiles inferred from $O_2(^1\Delta_g)$ measurements should be considered with caution above 85 km.

An example of the interaction of $O_2(^1\Delta_g)$ with the ionized atmosphere is its ionization by solar radiation in the wavelength region between 1027 and 1118 Å the ionization thresholds of $O_2(^3\Sigma_g^-)$ and $O_2(^1\Delta_g)$ respectively. Combining the ionization coefficients as given by Paulsen et al. (1972) with the actual values of the optical thickness and the $O_2(^1\Delta_g)$ concentration the O_2^+ production rate due to $O_2(^1\Delta_g)$ ionization can be derived. Besides the NO photoionization by Ly-α radiation this is believed to be the most important source of ions in the 70 to 90 km region.

Since the $O_2(^1\Delta_g)$ profile is strongly correlated to the O_3 profile it reflects not only the processes involving $O_2(^1\Delta_g)$ as one of the reactants but also those affecting the ozone concentration. The reaction

$$O+O_2+M \rightarrow O_3+M \tag{5}$$

is the only known source of O_3. Hence changes of the O concentration will directly influence the O_3 production rate. The reaction rate coefficient for (5) is according to Davis (1974) $k_2=1.1\ 10^{-34}\ exp\,(510/T)\ \mathrm{cm}^6\ \mathrm{s}^{-1}$. This means that a temperature change of $-50\ K$ which is not unrealistic at mesopause levels will enhance the O_3 production rate by a factor of 2.3 whereas the main destruction process for O_3 i.e. the photolysis remains unaffected. Anomalous structures in the temperature profile will therefore clearly show up in the O_3 and due to reaction (1) also in the $O_2(^1\Delta_g)$ profiles. Since the calculation of O_3 concentrations from Eq. (4) does not include the coefficient k_2 only poor knowledge of the temperature profile will nevertheless yield a relatively accurate O_3 profile. Therefore $O_2(^1\Delta_g)$ is a good indicator of both compositional and structural changes in the upper atmosphere especially for anomalous conditions such as winter anomaly events. While O_3 concentrations are not easily measured by other methods measurements of the emission height profile of the (0,0) band of $O_2(^1\Delta_g)$ is a simple and elegant way for determining the ozone content between 40 and at least 85 km. From this height on the O_3 values start to become less certain due to a lack of knowledge of the photochemistry involved but not due to the quality of the measured data.

2. Experiment

The experiment *DM* 2 for measuring the $O_2(^1\Delta_g)$ height profile was integrated in the payloads *B* II of the German Winter Anomaly and Trace Constituents Campaign.

The instrumentation comprised a simple filter radiometer and an electronic control and amplification unit. The principles of the radiometer are shown schematically in Figure 1. The bigger part of the instrument is a baffle system mounted in front of the actual radiometer housing. The radiation has to be thought to enter from the right. The optical layout is such that the entrance aperture at C which has a area of $3.14\ \mathrm{cm}^2$ is immaged by the system of the three lenses L_1, L_2, L_3 on the detector D the field of view beeing 0.314 *sr* or 5.7° half cone angle. The detector is a *PbS* element mounted upon a five-stage thermoelectric cooler which controls the temperature of the flake electronically to approximately $-30°$ C within a few hundredths of a degree, thus ensuring constant sensitivity and improved signal-to-noise ratio. A rotating chopper C just behind the entrance aperture generates a 107 Hz ac-voltage at the detector output. This signal is first ac amplified before it is rectified in a phase sensitive stage and then fed to three *dc*-amplifiers in parallel having amplification factors of 1, 10, and 100 respectively, thus giving a dynamical range of 2000 above

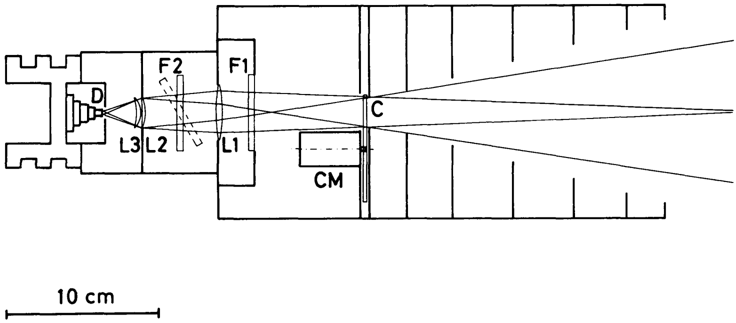

Fig. 1. Schematic drawing of the radiometer DM 2

noise levels. The noise equivalent radiance is $\pm 1.2\,10^{-9}\,W\,\mathrm{cm}^{-2} sr^{-1}$ or ± 100 kR as taken peak to peak. However, by smoothing the data noise can be reduced considerably.

The electronics includes further the control units for the chopper motor *CM* and the filter mechanism which tilts the filter F_2 once every second by means of two rotating magnets operating in turn in opposite directions. F_2 is an interference filter of 110 A half bandwidth. In the two positions normal and tilted to the optical axis the centre wavelengths are 1.266 μm and 1.244 μm respectively. The transmission efficiency for the $O_2(^1\Delta_g)$ band is 0.75 and 0.01 respectively. Thus, discrimimation of band emission against background radiation is possible. F_1 is an additional blocking filter for suppressing short wavelength radiation produced by Rayleigh scattering of sunlight.

In order to derive $O_2(^1\Delta_g)$ number densities it is necessary to measure the emission in absolute units. Therefore the instruments were calibrated in the laboratory. Neither recalibration prior to launch nor inflight checks of the sensitivity of the radiometer were considered to be necessary since changes of the calibration with time had shown to be beyond detectable limits. The calibration was done in two steps. First the relative response of the radiometer as a whole was measured in the two filter passbands using a monochromator as a source and a thermopile for comparison. Assuming the spectral response of the thermopile to be independent of wavelength between 1.1 and 1.4 μm it is possible to calculate the spectral response of the radiometer. The second step was the absolute calibration against a blackbody. The emissivity from the viewpoint of geometry of the source and the emissivity of wall painting used should be better than 0.99. The temperature of the cavity was controled by an electronic unit by means of three separate electric heating circuits within $\pm 0.1\ K$ at a preset value which in turn was monitored by a calibrated Pt thermometer. Hence the overall blackbody calibration should be accurate to a few percent.

The radiometer was installed in the rocket looking from the aft end parallel to the payload axis. After motor separation an attitude control system was to turn the playload over and to control its attitude in a way that the axis was closely aligned to the tangent of the trajectory on the downleg portion of the flight. Soon after apogee an optical shutter inside the radiometer was opened by a timer signal and the instrument started measuring down to approtimately 40 km where the payload began to tumble in an uncontrolled manner. Since the rockets were fired to the southwest late in the afternoon the sun was off the optical axis of the radiometer more than 90° for the whole time of the measurement.

There were actually two flights of the instrumentation from Arenosillo, Spain on January 4, 1976 15:30 UT and on January 21, 1976 15:30 UT. Both flights took place during winter anomalous conditions. Due to a failure of an electronic part shortly after take-off on the second launch evaluable data could only be gathered during the first flight.

3. Results

As an example of the data obtained during the flight on January 4, 1976 Figure 2 shows the signal vs. height as measured in the filter channel at 1.266 μm. The profiles of both signal channels were submitted to a smoothing procedure using cubic spline functions. The $O_2(^1\Delta_g)$ band emission and the background radiation

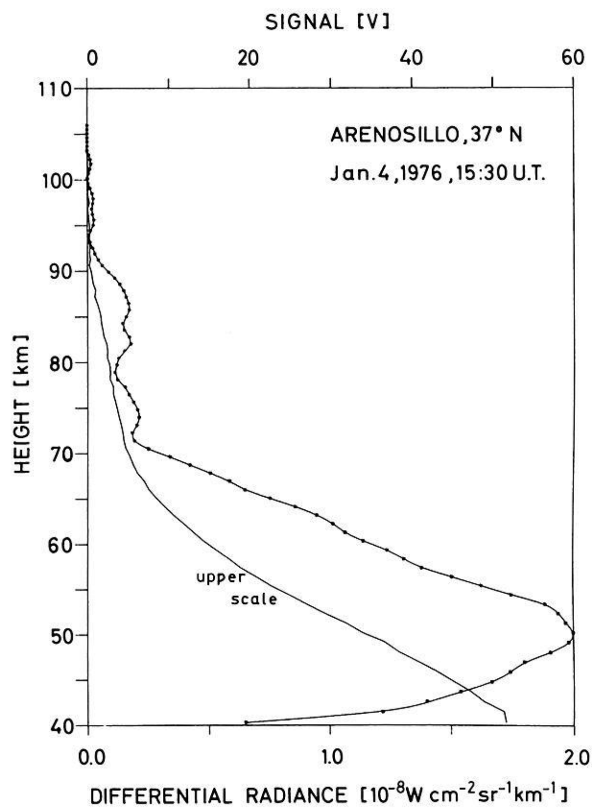

Fig. 2. Unsmoothed signal as measured in the 1.266 μm channel versus height (upper scale) and $O_2(^1\Delta_g)$ differential radiance profile (lower scale)

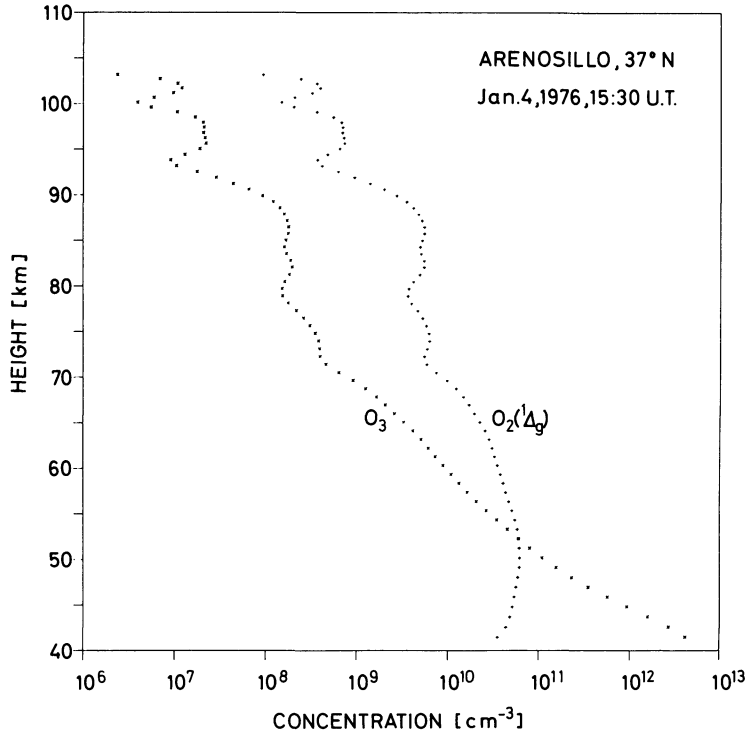

Fig. 3. Concentration height profiles of $O_2(^1\Delta_g)$ and O_3

were separated by solving the set of two equations for each set of data points. For this purpose the actual transmission of the filters for the lines of the band have to be calculated at each of the height levels using the temperature of the emitting layers weighted by the number densities of $O_2(^1\Delta_g)$ in it. This was achieved in a couple of iterations starting from some model profile for $O_2(^1\Delta_g)$ and then using the calculated $O_2(^1\Delta_g)$ values for the next run. The temperature data used here were in part those deduced from the scale heights of the N_2 density profile measured by experiment *DH* 2 flown in payload B IV 1 h in advance of *B* II. For altitudes below 57 km the data were taken from the measurement of a Spanish INTA rocket launched 10 min after *B* II. The obtained values of the integrated radiance of the band were then corrected to zenith and differentiated with respect to height to give the differential radiance or volume emission rate profile shown also in Figure 2. The concentration or number density profile was obtained by dividing the volume emission rates given in photon units by the Einstein transition factor. The ozone profile was then calculated according to Eq. (4) using the data of experiment *DH*2 above 80 km and CIRA 1972 data below for the atmospheric density. The two profiles of $O_2(^1\Delta_g)$ and O_3 are given in Figure 3.

There are some remarkable differences in comparison to results of other experiments. The total overhead intensity of the $O_2(^1\Delta_g)$ band of 34 *MR* as well as the volume emission rate of 1.6 MR/km at 50 km are considerable higher than the values reported by Evans et al. (1968) and Evans and Llewellyn (1970). Besides, there are distinct secondary minima at 72, 93, and 100 km. As pointed out earlier both the $O_2(^1\Delta_g)$ and the O_3 densities should reflect structures in the temperature profile. There were in fact extraordinary deviations from the CIRA 1972 temperature profile for January 40° N. At the time of the flight there was a stratospheric warming over southwest Europe. In the mesosphere, however, the combined data of INTA and experiment $DH2$ seem to indicate a wavelike structure in the temperature profile showing minima near 60, 85, and 98 km and maxima near 72 and 92 km the deviations being 30 to 50 K either way. The correlation between the temperature profile on one side and the $O_2(^1\Delta_g)$ and O_3 profiles on the other is striking. But also the magnitude of the deviations seems to be reasonable. For example, the decrease of nearly 50 K around 85 km can well explain the observed enhancement by a factor of 2 in the O_3 content as compared to the observation of Miller and Ryder (1973). However, according to theoretical studies by Fukuyama (1974) and Koshelev (1976) differences of this order could also be attributed to the different latitude and season at which the measurements were conducted.

Below 52 km the scale height of the O_3 profile changes drastically from the normal 4.4 km to 2.0 km indicating a marked increase of the O_3 content in the stratosphere. This increase seems to be related to the observed stratospheric warming which might at least partially be produced by enhanced absorption of solar radiation in the Hartley band of ozone. It should be pointed out that the temperature data used here are not to be considered as final at present. Hence, the presented results are also preliminary although only minor changes are to be expected for the $O_2(^1\Delta_g)$ and O_3 profiles.

Acknowledgment: This research was sponsored by the Bundesministerium für Forschung und Technologie under contract RV 14-B 103/73-B II/DM2. The radiometer was built at the Meteorologisches Institut der Universität München. The electronics was developed by the Institut für Nachrichtentechnik der Deutschen Forschungs- und Versuchsanstalt für Luft- und Raumfahrt, Oberpfaffenhofen. The authors are grateful to Prof. H.-J. Bolle for his support of the project.

References

Ackerman, M.: Ultraviolet solar radiation related to mesospheric processes. In: Mesospheric models and related experiments, G. Fiocco, ed., pp. 149–159. Dordrecht-Holland: Reidel 1971

Badger, R.M., Wright, A.C., Whitlock, R.F.: Absolute intensities of the discrete and continous absorption bands of oxygen gas at 1.26 μ and 1.065 μ and the radiative lifetime of the $^1\Delta_g$ state of oxygen. J. Chem. Phys. **43**, 4345–4350, 1965

CIRA 1972: COSPAR International Reference Atmosphere 1972, Berlin: Akademie-Verlag 1972

Clark, I.D., Wayne, R.P.: Collisional quenching of $O_2(^1\Delta_g)$. Proc. Roy. Soc. London A **314**, 111–127, 1969

Davis, D.D.: A kinetics review of atmospheric reactions involving H_xO_y compounds. Can. J. Chem. **52**, 1405–1414, 1974

Evans, W.J., Hunten, D.M., Llewellyn, E.J., Vallance Jones, A.: Altitude profile of the Infrared Atmospheric System of oxygen in the dayglow. J. Geophys. Res. **73**, 2885–2896, 1968

Evans, W.J., Llewellyn, E.J.: Molecular oxygen emissions in the airglow. Ann. Géophys. **26**, 167–178, 1970

Fukuyama, K.: Latitudinal distribution of minor neutral hydrogen-oxygen constituents in the winter mesosphere and lower thermosphere. J. Atmospheric Terrest. Phys. **36**, 1297–1320, 1974
Gattinger, R.L., Vallance Jones, A.: The $^1\Delta_g - ^3\Sigma_g^- O_2$ bands in the twilight and day airglow. Planetary Space Sci. **14**, 1–10, 1966
Koshelev, V.V.: Diurnal and seasonal variations of oxygen, hydrogen, and nitrogen components at heights of mesosphere and lower thermosphere. J. Atmospheric Terrest. Phys. **38**, 991–998, 1976
Miller, D.E., Ryder, P.: Measurement of ozone concentration from 55 to 95 km at sunset. Planetary Space Sci. **21**, 963–970, 1973
Paulsen, D.E., Huffman, R.E., Larrabee, J.C.: Improved photoionization rates of $O_2(^1\Delta_g)$ in the *D* region. Radio Sci. **7**, 51–55, 1972
Vallance Jones, A., Harrison, A.W.: $^1\Delta_g - ^3\Sigma_g^- - O_2$ infrared emission band in the twilight airglow spectrum. J. Atmospheric Terrest. Phys. **13**, 45–60, 1958

Received May 2, 1977